Assessment and Improvement of CLM4.5 in Simulation of Land Surface Temperature in Mainland China

yulong Ren[1]

[1]Institute of Arid Meteorology, CMA

November 24, 2022

Abstract

Land surface temperature(LST) is the key indicators to assess land surface models (LSMs). CLM4.5 has attracted much attention in mainland China. However, there have been few comprehensive LST assessments of CLM4.5 that used abundant latest long-term observation data from mainland China and considered land-atmosphere coupling. Therefore it is difficult to evaluate its performance for an actual climate simulation. In this work, LST data from the recent 30 years were collected from 809 Chinese meteorological stations, and the simulation capability of CLM4.5 for LST was comprehensively assessed for the first time. Then, in order to improve the model, sensitivity tests of soil thermal conductivity (STC) were carried out. Although CLM4.5 could accurately simulate the spatial distribution character of LST, there was a cold bias of 4.5{degree sign}C for all of mainland China. Seasonally, larger bias was observed in summer and autumn, which had more precipitation and greater soil moisture than other seasons. Deviation increased from southeast to northwest, but varied greatly between seasons. There was a significant linear regression relationship between two LSTs, with annual correlation coefficients of the two LSTs for all stations between 0.75 and 0.9 ($P < 0.001$). LST increased at a rate of 0.058{degree sign}C/a. Though it was successfully simulated, the trend value was smaller. The bias of CLM4.5 was better than that of ERA-interim but slightly worse than that of ERA-interim/Land. Assessment of three different STC schemes showed that the Lu-Ren scheme was the most one that suitalbe for LST siumulation in mainland china.

Assessment and Improvement of CLM4.5 in Simulation of Land Surface Temperature in Mainland China

Y. L.Ren[1]

[1]Institute of Arid Meteorology, CMA, Key Laboratory of Arid Climatic Change and Reducing Disaster of Gansu Province, Key Laboratory of Arid Climate Change and Disaster Reduction of CMA,730020,China.

Corresponding author: Ren YuLong(ryl@iamcma.cn & yulongren731100@163.com)

Key Points:

- Considering land–atmosphere coupling,the longest and latest observed Land surface temperature(LST) dataset for mainland China was used for the first time to comprehensive assess LST in that region as simulated by CLM4.5.
- There are systematic cold deviations in the simulation of land surface temperature in mainland China by CLM4.5. There was a significant linear regression relationship between two LSTs. Though the trend of the LST varation was successfully simulated, the value was smaller than that of observation.
- We added a new scheme of soil thermal conductivity that more suitalbe for LST siumulation in mainland china, which has made CLM4.5 get further development in Chinese mainland.

Abstract LST is the key indicators to assess land surface models (LSMs). Common Land Model 4.5 (CLM4.5) has attracted much attention in mainland China. However, there have been few comprehensive LST assessments of CLM4.5 that used abundant latest long-term observation data from mainland China and considered land–atmosphere coupling. Therefore it is difficult to evaluate its performance for an actual climate simulation. In this work, LST data from the recent 30 years were collected from 809 Chinese meteorological stations, and the simulation capability of CLM4.5 for LST was comprehensively assessed for the first time. Then, in order to improve the model, sensitivity tests of soil thermal conductivity (STC) were carried out. Although CLM4.5 could accurately simulate the spatial distribution character of LST, there was a cold bias of 4.5°C for all of mainland China. Seasonally, larger bias was observed in summer and autumn, which had more precipitation and greater soil moisture than other seasons. Deviation increased from southeast to northwest, but varied greatly between seasons. There was a significant linear regression relationship between two LSTs, with annual correlation coefficients of the two LSTs for all stations between 0.75 and 0.9 ($P < 0.001$). LST increased at a rate of 0.058°C/a. Though it was successfully simulated, the trend value was smaller. The bias of CLM4.5 was better than that of ERA-interim but slightly worse than that of ERA-interim/Land. Assessment of three different STC schemes showed that the Lu-Ren scheme was the most one that suitalbe for LST siumulation in mainland china. To develop a new STC scheme considering the role of water vapor is an effective way for improving the model in mainland China.

Plain Language Summary LST is an important indicator to evaluate the performance of Land Surface Model(LSM)−one of the major components of Regional Climate Models(RCMs). Although the third generation LSM CLM4.5 has been extensively studied in mainland China, its simulated performance has not been systematically evaluated due to the lack of observational LST data, which has affected the improvement of the model. In this paper, by considering land-atmosphere interaction, the latest LST dataset including 809 sites in mainland China are first used to evaluate the LST simulation capability of CLM4.5 comprehensively. Based on the physical model for calculating LST in CLM4.5, three numerical experiments on STC schemes were carried out and the result has reveal the best STC scheme for the Chinese mainland. Then, a new scheme of STC in CLM4.5 was added and it is verified to be useful, which has made further development of CLM4.5 in Chinese mainland.

1.Introduction

Changes of land surface temperature (LST) can alter the balance of energy and material between land and atmosphere, and cause major changes in precipitation, temperature, vegetation and ecological processes (Wilson et al. 2003; Zhong et al. 2011). Thus, it is an important indicator for studying global climate change (Wan and Li 1997; Coll et al. 2016; Duan et al. 2017; Jones and Trewin 2015). LST is calculated by a land surface model (LSM) that provides necessary lower boundary conditions for regional climate models (RCM). The accuracy of that calculation has a direct impact on soil water, heat, and ecological process simulation. Therefore, it is also one of the main indicators to assess LSM performance.

LSM has undergone three generations of development. After the 1st-generation box model and 2nd-generation model considering vegetation physiological and physical processes, the LSM has developed into its 3rd generation, considering biochemical effects of the carbon cycle. The Community Land Model (CLM) (Zeng et al. 2002) developed by the National Center for Atmospheric Research (NCAR) in the United States, based on 2nd-generation LSMs such as

BATS, IAP94 and NCAR-LSM, is a typical 3rd-generation LSM. It has 10 uneven soil layers, 5 snowfall layers, and 1 vegetation layer. The data of land surface cover include soil color, soil texture, percent coverage of plant functional types (PFTs) per grid, leaf and stem area indexes. CLM classifies surface vegetation into 17 PFTs. Each grid point can contain 17 different PFTs, which are treated as the percentage of each PFT area to the grid area. This includes physical, chemical, hydrological and biochemical processes such as biogeophysics, the hydrologic cycle, biogeochemistry, and dynamic planting related to climate change (Hoffman et al. 2004). It has developed rapidly across versions CLM2.0, CLM3.0, CLM3.5 and CLM4.0. CLM4.5 is the latest released version, which revises the photosynthesis scheme, improves hydrologic processes and the wetland distribution in cold regions, and includes new parameterization schemes of snow cover, lake model, crop model, and various city types. In addition, a nitrogen fixation mechanism and methane emission model in the soil vertical direction have been introduced. Since the release of this LSM, it has been widely applied in ecology (Tang et al. 2015; Duarte et al. 2017; Bilionis et al. 2014; Chen et al. 2018; Peng et al. 2018; Brunke et al. 2016; Wu and Dickinson 2004), climate change (Umair et al. 2018; Lawrence et al. 2012), assessment of the role of greenhouse gases (Zhang et al. 2016; Zhang and Wang 1997; Akkermans et al. 2014), and hydrology (Fu et al. 2016; Liu et al. 2017; Hack et al. 2006). It is considered one of the most developed and potentially useful LSMs in the world (Lai et al. 2014).

The model has also been used in studies on the simulation and assessment of LST in mainland China (Meng et al. 2017; Wang et al. 2015; Song et al. 2014; Wang et al. 2015). Sun et al. (2017) drove CLM3.5 based on CLDAS (CMA Land Data Assimilation System) atmospheric driving data, using LST from ground observation stations to assess the quality. The results show that the bias and root-mean-square error (RMSE) of simulated LST vs. observed data varied seasonally. Further, the bias and RMSE of simulated LST vs. observed data were smaller in eastern China than in its west. Meng et al. (2017) found that the CLM3.5 model had the greatest difference between simulated and observed LSTs in Xinjiang, with a maximum difference of ~5 K in July each year. Guo et al. (2017) used NCEP atmospheric forcing data to drive CLM4.5 for simulating changes of soil temperature on the Tibetan Plateau over the past century. The simulation results were validated by observation data of soil temperature from meteorological stations and field borehole monitoring stations. The results show that CLM4.5 could reasonably simulate observed changes of soil temperature on the plateau. Chen et al. (2010) used CLM3.0 and global atmospheric near-surface forcing data from Princeton University to conduct offline simulation experiments on soil temperature in China from 1948 to 2001, further assessing the capability of CLM3.0 to simulate soil temperature at different levels. The results show that the model could simulate the spatial distribution of multiyear average soil temperature in the country. The simulated soil temperature was generally lower than observed except for some areas where the simulated values were larger than observed. The model could well-reflect the interannual variation of soil temperature in China. Moreover, the model could basically grasp the trend of that temperature, but the simulated trend was weaker than observed. Xie et al. (2017) used observation data from Nagqu Station of Plateau Climate and Environment of the Chinese Academy of Sciences to assess model simulation performance for surface energy exchange at the underlying surface of an alpine meadow on the Tibetan Plateau. The results showed that CLM4.5 could effectively simulate seasonal variations and diurnal cycles of surface longwave, reflected and net radiations; sensible and latent heat fluxes; and surface soil heat fluxes during non-freezing periods in spring, summer and autumn on the plateau. However, the simulation of LST during the winter freezing period gave values smaller than observed.

Nevertheless, most evaluations only had a few LSM stations with short observation periods. But the Chinese mainland is vast and its land surface characteristics vary substantially by region. Therefore, the associated conclusions lack spatial and temporal representativeness. In addition, land–atmosphere interaction feedback has a major impact on LST calculation. Most assessments considered only the forcing effect of the atmosphere on the land surface, neglecting the transport of energy and mass from that surface. Therefore, it is difficult to fully evaluate the performance of CLM4.5 for an actual climate simulation. All of these limit the development of CLM4.5 for mainland China. To solve these problems, we designed a long-term (30 years) numerical simulation test of LST for mainland China on the basis of long-term observational LST data. Finally, the experiment of improving soil thermal conductivity model was carried out. The results will promote the development of CLM4.5 in mainland China.

2 Materials and Methods

2.1 Regional Climate Model version 4.6 (RegCM 4.6)

Regional Climate Model version 4.6 (RegCM 4.6) was used to provide atmospheric forcing fields. RegCM is a regional climate model established by Dickinson and Giorgi in the late 1980s through expansion and modification of the radiation scheme, convection parameterization scheme, and land surface physical process in mesoscale model MM4 (Dickinson et al. 1989; Giorgi and Bates 1989). Giorgi et al. subsequently produced RegCM2, RegCM3 and RegCM4 by improving the physical process scheme and mesoscale model (Giorgi et al. 1993; Giorgi et al. 1993). RegCM4.6 is the latest mature version. In this version, a MM5 non-static dynamic frame option is added, which improves model spatial resolution to 10 km and updates the radiation and convection parameterization schemes. RegCM is the most widely used regional climate model in China. It is not only used for climate simulation and diagnosis but is also one of the supporting tools for climate prediction.

2.2 Soil Thermal Conductivity (STC)

The calculation model of soil temperature used in CLM4.5 is as follows.

$$c\frac{\partial T}{\partial z} = \frac{\partial}{\partial z}\left(\lambda\frac{\partial T}{\partial z}\right) \qquad (4)$$

Here, T is soil temperature (K), z is downward in the vertical direction (m), c is the snow/soil heat capacity (J m^{-3} K^{-1}), t is time (s), and λ is the STC (W m^{-1} K^{-1}). The results show that λ had a great influence on the calculation of soil temperature. In CLM4.5, the model proposed by Johansen (1975) was used for the calculation of λ. This is a semi-theoretical and semi-empirical model for calculating λ. Its expression is

$$\lambda = \left(\lambda_{sat} - \lambda_{dry}\right) \cdot K_e + \lambda_{dry} \qquad (5)$$

Here, $\boldsymbol{\lambda_{sat}}$ is the thermal conductivity for saturated soil, $\boldsymbol{\lambda_{dry}}$ is the thermal conductivity for dry soil, and $\boldsymbol{K_e}$ is the Kersten constant, whose expression in this model is

$$K_e = \begin{cases} 0.7\,log\,S_r + 1.0, 0.05 < S_r \le 0.1 \\ log\,S_r + 1.0, \qquad S_r > 0.1 \end{cases} \qquad (6)$$

where $\boldsymbol{s_r}$ is the saturation of soil. Results (Su et al. 2016) have shown that $\boldsymbol{K_e}$ in the model is logarithmic, and the calculated $\boldsymbol{\lambda}$ was clearly smaller than the measured value. To overcome this problem, Côté and Konrad (2005) proposed a new expression of $\boldsymbol{K_e}$:

$$K_e = \frac{kS_r}{1+(k-1)S_r} \tag{7}$$

where k is a parameter related to soil texture. To make the Johansen model more suitable for low soil moisture content, Lu and Ren (2006) proposed a new scheme:

$$\boldsymbol{K_e = \exp\left(\alpha(1 - S_r^{\alpha-1.33})\right)} \tag{8}$$

where $\boldsymbol{\alpha}$ is a parameter related to soil texture.

2.3 Major assessment indicators

(1) Bias

$$\boldsymbol{BIAS = \frac{1}{n}\sum_{i=1}^{n}(S_i - O_i)} \tag{1}$$

Here, *Si* is the simulated element (such as precipitation and temperature); *Oi* is the corresponding observed element, which can be used to test whether simulated values from the model are large or small as well as the corresponding magnitude.

(2)RMSE

$$\boldsymbol{RMSE = \sqrt{\frac{\sum_{i=1}^{n}\left(X_{obs,i} - X_{model,i}\right)^2}{n}}} \tag{2}$$

This reflects the deviation of simulated from observed data. The smaller the value, the greater the simulation accuracy and the better the performance.

(3)Pearson correlation coefficient

$$\boldsymbol{r = \frac{\sum_{i=1}^{n}(x_i - \overline{x})(y_i - \overline{y})}{\sqrt{\sum_{i=1}^{n}(x_i - \overline{x})^2}\sqrt{\sum_{i=1}^{n}(y_i - \overline{y})^2}}} \tag{3}$$

This is a statistical quantity reflecting the linear correlation of two variables. The larger the absolute value, the stronger the correlation.

2.4 Design of Numerical Experiment

The simulation area is shown in Fig. 1. The latitude range was 15.76–57.36°N and longitude range 66.25–141.13°E. There were 160 grid points in latitude and 145 in longitude. The horizontal grid size was 30 km, and the vertical was divided into 23 layers. ERA-Interim reanalysis data from January 1987 to December 2017 were used for the lateral boundary. The data had a horizontal resolution of 0.75° × 0.75° (~80 km), 37 layers in the vertical, and a temporal resolution of 6 hours. Sea surface temperature data were OSSST monthly average data of NOAA from the same period. Model parameters are listed in Table 1.

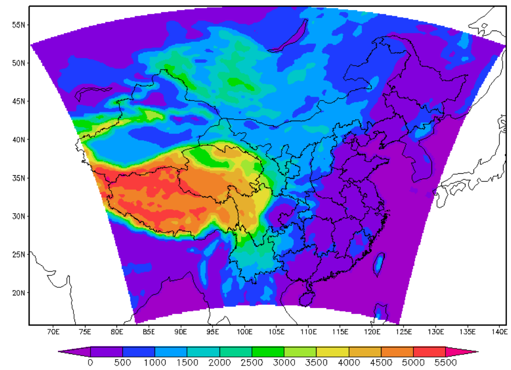

Fig1. The simulation area. Shadow represents terrain height in m

Table.1 Main simulation parameters

Dynamic structure	Test scheme
Dynamic frame	MM5 non-static frame
Large-scale precipitation scheme	SUBEX (Subgrid explicit water vapor scheme)
Radiation transmission scheme	NCAR CCM3
Sea surface flux scheme	Zeng
Pressure gradient scheme	Hydrostatic recursion

As in Fig.2,mainland China was divided into four regions (Huang 1989): (1) the northern region is the northern part of China with a monsoon climate. (2) The southern region is south of the Qinling-Huaihe River and east of the Tibetan Plateau. It faces southeast to the East China Sea and South China Sea, includes the middle and lower reaches of the Yangtze River, the southern coast and southwest provinces (cities and autonomous regions), and is the southern part of China with a monsoon climate. (3) The northwestern region is generally west of the Great Khingan Range and north of the Great Wall and Kunlun-Altun Mountains. It embraces the non-monsoon climate portions of Inner Mongolia, Xinjiang, Ningxia and northwestern Gansu. (4) The Tibetan Plateau.

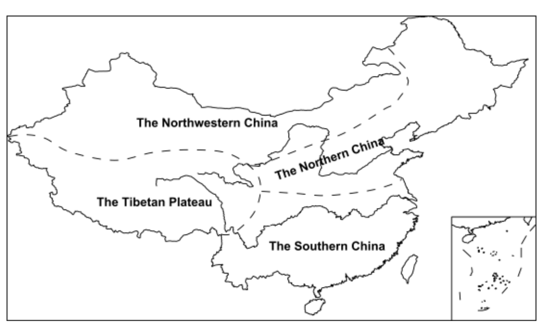

Fig 2. Four natural regions in mainland China

3 Data

3.1 Observation data of LST

Observed data of LST in mainland China were collected from the daily climate dataset of Chinese ground international exchange stations compiled by the China Meteorological Administration. The dataset contains daily data of meteorological elements from China reference and basic meteorological stations since January 1951. During dataset construction, repeated quality detection and control measures were applied to the observation data, thereby correcting a large number of erroneous data. Furthermore, digitized missing data were entered, suspicious and erroneous data found were manually verified and corrected, and quality control codes were labeled for all element data. These steps substantially improved data quality. To ensure data reliability, we used daily observed LST data from the 30-year study period (January 1, 1988 to December 31, 2017).

3.2 Reanalysis data of ERA-Interim and ERA-Interim/Land

ERA-Interim is the latest global atmospheric reanalysis dataset from the European Centre for Medium-Range Weather Forecasts (ECMWF). Using advanced 4Dvar variational assimilation system Cy31r2, ERA-Interim assimilates satellite brightness temperature, scatterometer, satellite inversion of the atmospheric motion state, GPS occultation, satellite inversion of ozone, and conventional observations. It is one of the highest-quality reanalysis datasets in the world. ERA-Interim/Land is a reanalysis dataset of atmospheric forcing fields using the ECMWF land surface model, Hydrology Tiled ECMWF Scheme for Surface Exchange over Land, and ERA-Interim. Global Precipitation Climatology Project version 2.1 was used as the reanalysis dataset of land surface parameters, generated after precipitation adjustment. ERA-Interim/Land provides comprehensive and consistent estimates of the global water resource and is used to initialize numerical weather forecasting and climate models (Balsamo et al. 2015; Albergel et al. 2013).

4 Results

4.1 Simulation of CLM4.5 for LST

4.1.1 Bias

The analysis of annual average LST in mainland China showed that it decreased gradually from the southeast coast to interior northwest. The annual average LST of the southeast coast was > 20°C and that between the Yangtze and Yellow rivers was about 15°C. That of most areas in North China was 5–10°C. LST of the Tibetan Plateau was the coolest, with most areas < 5°C. LST from northern Xinjiang to the southern Xinjiang Basin increased from 10°C to 15°C (Fig. 3a). CLM4.5 showed favorable simulation performance in the spatial variation of annual average LST in China. The LST decrease from the southeast coast to interior northwest was accurately simulated(Fig. 3b). However, simulated values were clearly smaller than observed, which most regions had a cold bias > 2°C. Specifically, there was a cold bias of ~2–4°C east of 105°E, 6–8°C west of 105°E, and 4–6°C in other regions (Fig. 3b).

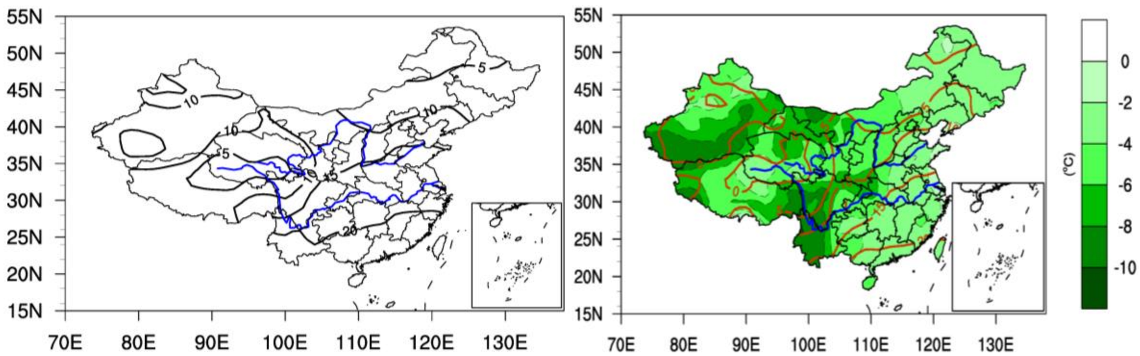

(a) (b)

Fig 3. The observed and simulated LST and the bias: (a) observation; (b) simulation; (c) bias; unit: °C.

The simulations of average LST in the four seasons were very similar to the observed, with a decreasing trend from southeast to northwest. CLM4.5 showed good simulation performance for this spatial distribution, but the bias varied greatly seasonally (data not shown). In spring, the bias was smallest in southern China. There, a cold bias of 2–4°C was most common, with some areas having a cold bias of 0–2°C. There was a cold bias of 6–8°C in most of northern and northwestern China and the Tibetan Plateau (Fig. 4a). In summer, except for some parts of southwestern and southern China where there was a cold bias of 4–6°C, bias in other regions was large (> 6°C). The Tibetan Plateau had a cold bias of > 8°C (Fig. 4b). In autumn, there was a cold bias of 2–4°C east of 105°E, 6–8°C west of that meridian, and 4–6°C in North China and some of the plateau (Fig. 4c). In winter, the simulated bias of all regions in China decreased considerably. Except for the simulated bias (~6°C) in southwestern China, that in most regions was < 4°C (Fig. 4d).

Analyzing the climatic background, summer and autumn are the principal rainy seasons in China because they are strongly affected by the East Asian summer monsoon. Precipitation in most of mainland China was heavy, which increased soil moisture. Winter and spring were controlled by a single westerly circulation system. Precipitation was weak and soil moisture decreased in most of the mainland. This indicates that the bias was closely related to soil moisture.

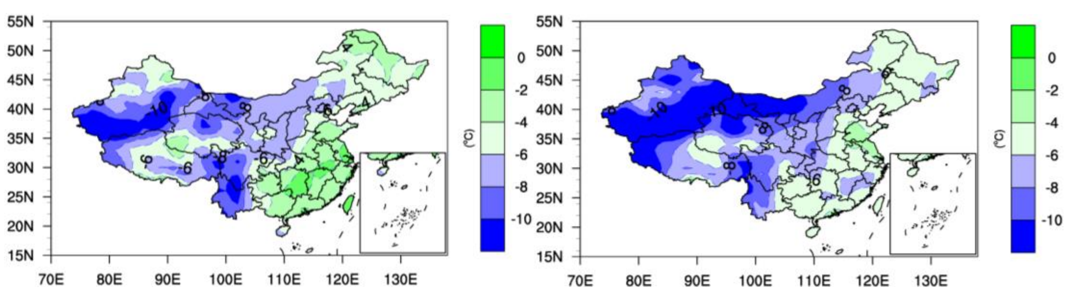

(a) (b)

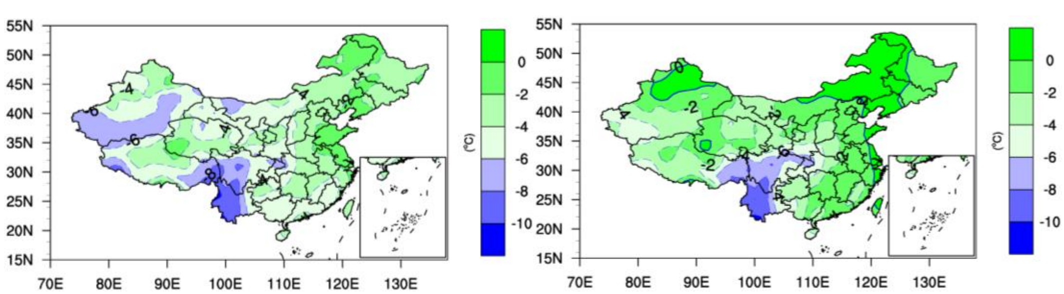

(c) (d)

Fig 4. Bias for (a) spring, (b) summer, (c) autumn, and (d) winter; unit: °C

There were clear regional differences and seasonal variations (Fig. 5) in the bias of CLM4.5 for LST. For the regional difference, bias was small in the southern and northern regions, with an average annual cold bias of ~4°C. Bias in the northwestern region was large, with an average annual cold bias of ~5.5°C. Bias of the Tibetan Plateau was the greatest, with an average annual cold bias of ~6°C. For seasonal variation, the plateau region had the largest bias in spring. Summer bias was maximum in other regions. Summer cold bias in the northwestern region was ~9°C, and that in the northern and southern regions was ~5°C. In winter, the bias was small in all regions. The cold bias in the northwestern and northern regions was ~2°C. The cold bias in the plateau region was maximum (~4°C). ERA-Interim and ERA-Interim/Land exhibited bias similar to that of CLM. ERA-Interim/Land had the smallest bias. The bias of ERA-Interim was similar to that of CLM4.5, and the latter showed the smallest bias in the Tibetan Plateau region.

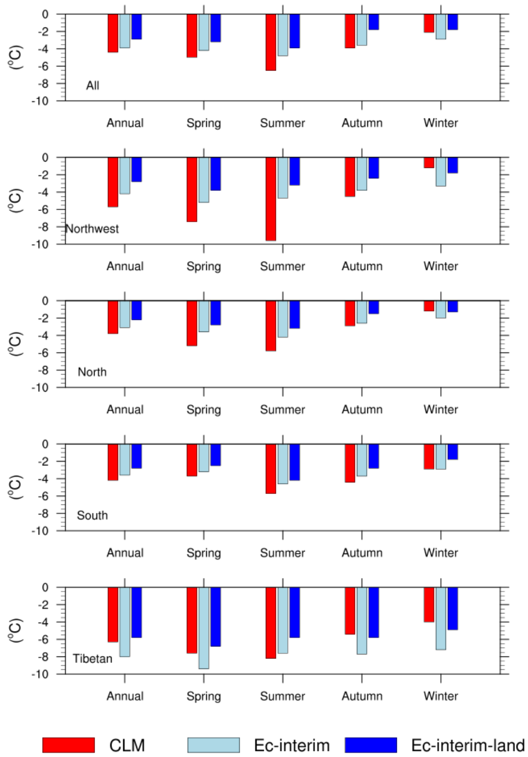

Fig 5. Bias in (a) all areas, (b) northwest, (c) north, (d) south, and (e) Tibetan; unit: °C.

4.1.2 RMSE

The annual RMSE analysis showed that the RMSE in mainland China increased gradually from southeast to northwest. The RMSE of most of the southern regions was 1–3°C, with that of most of the northern regions at 5–7°C. That of the eastern part of the northwestern region was 7–9°C and that of the southern Xinjiang Basin was 9–11°C. That of the plateau was 3–11°C (Fig. 6a). In spring, the RMSE in China was relatively large. There was again a decrease from southeast to northwest. The RMSE of most of the southern regions was < 5°C, whereas that of other regions was 9–11°C (Fig. 6b). Summer and autumn had the minimum RMSE among the four seasons.

Except for the plateau region where the RMSE was 9–11°C, Chinese regions had 3–5°C (Fig. 6c and d). The RMSE distribution in winter was similar to that of the entire year (Fig. 6e).

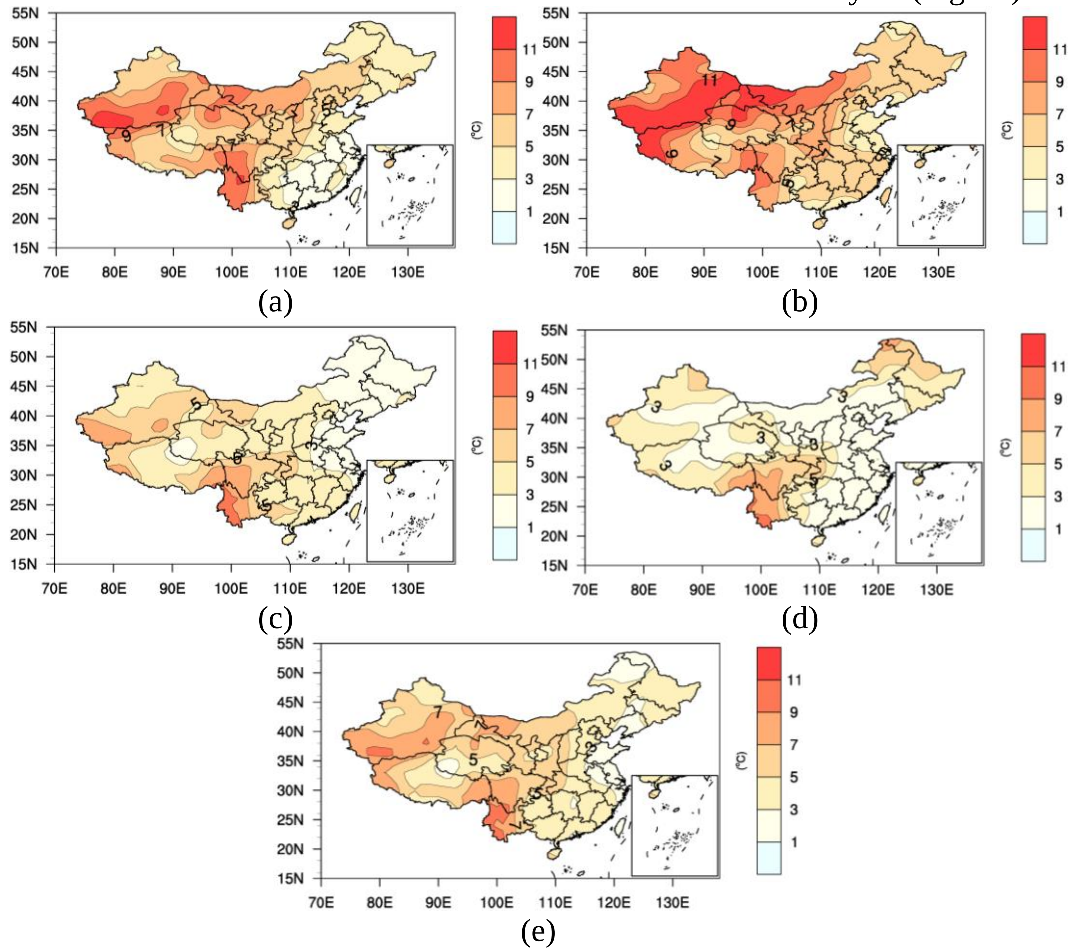

Fig 6. RMSE in (a) all year, (b) spring, (c) summer, (d) autumn, and (e) winter, unit: °C.

The RMSE of CLM4.5 also showed clear regional differences and seasonal variations. Regarding the former, the RMSE in the northern and southern regions was small (< 4°C), followed by the northwestern region (4–5°C). That of the Tibetan Plateau was the largest (~7°C). For seasonal variation, the smallest RMSE was observed in summer and autumn, with the largest in winter and spring. The RMSE of CLM4.5 was slightly smaller than that of ERA-Interim, with ERA-Interim/Land having the minimum RMSE(Fig.7).

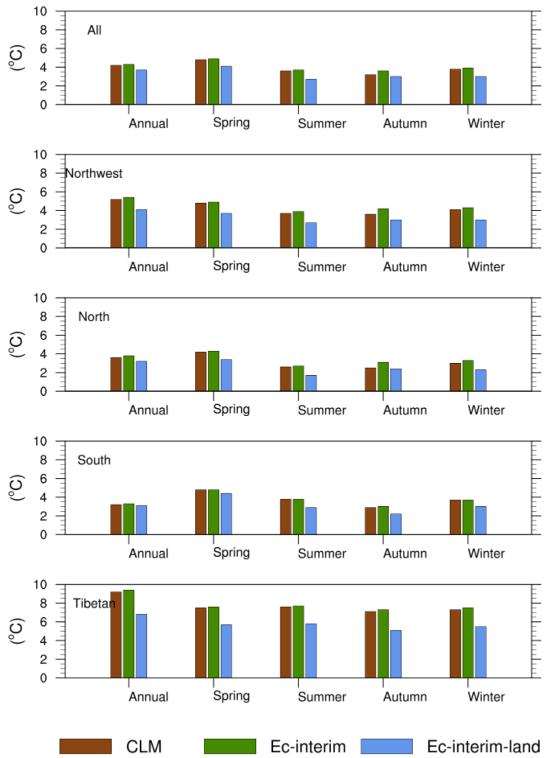

Fig 7. RMSE in different seasons and areas, unit: °C.

4.1.3 Simulation of LST Change

1) Correlation

Correlation coefficients between simulation and observation LST at all stations in China were between 0.75 and 0.9 ($P < 0.001$). The largest correlation coefficient was observed in summer, between 0.70 and 0.85 ($P < 0.001$). The next largest correlation coefficient was in autumn(0.5–0.75, $P < 0.001$). The results in spring are similar to those in autumn. and its maximum correlation coefficient was 0.80 ($P < 0.001$). The coefficient was between 0.35 and 0.65 in winter ($P < 0.05$), respectively (Fig. 8).

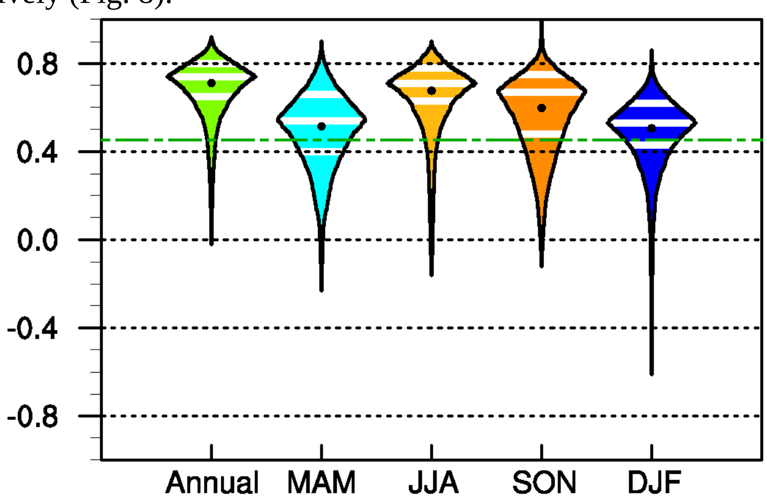

Fig 8. Correlation between observed and simulated LST. The green line showed that the correlation coefficient reached the significance level of $\alpha = 0.01$.

Regression of the regional average LST simulated by CLM4.5 with the observed showed that annual and seasonal predictions were linearly correlated with observed values. Except for the wide prediction area for winter, the 95% prediction interval for each season was narrow and the 95% confidence level was reached at most points. In addition, the LST simulated by CLM4.5 was ~4–5°C lower than observed (Fig. 9a–e). The above analysis shows that CLM4.5 could effectively simulate the trend of LST in mainland China.

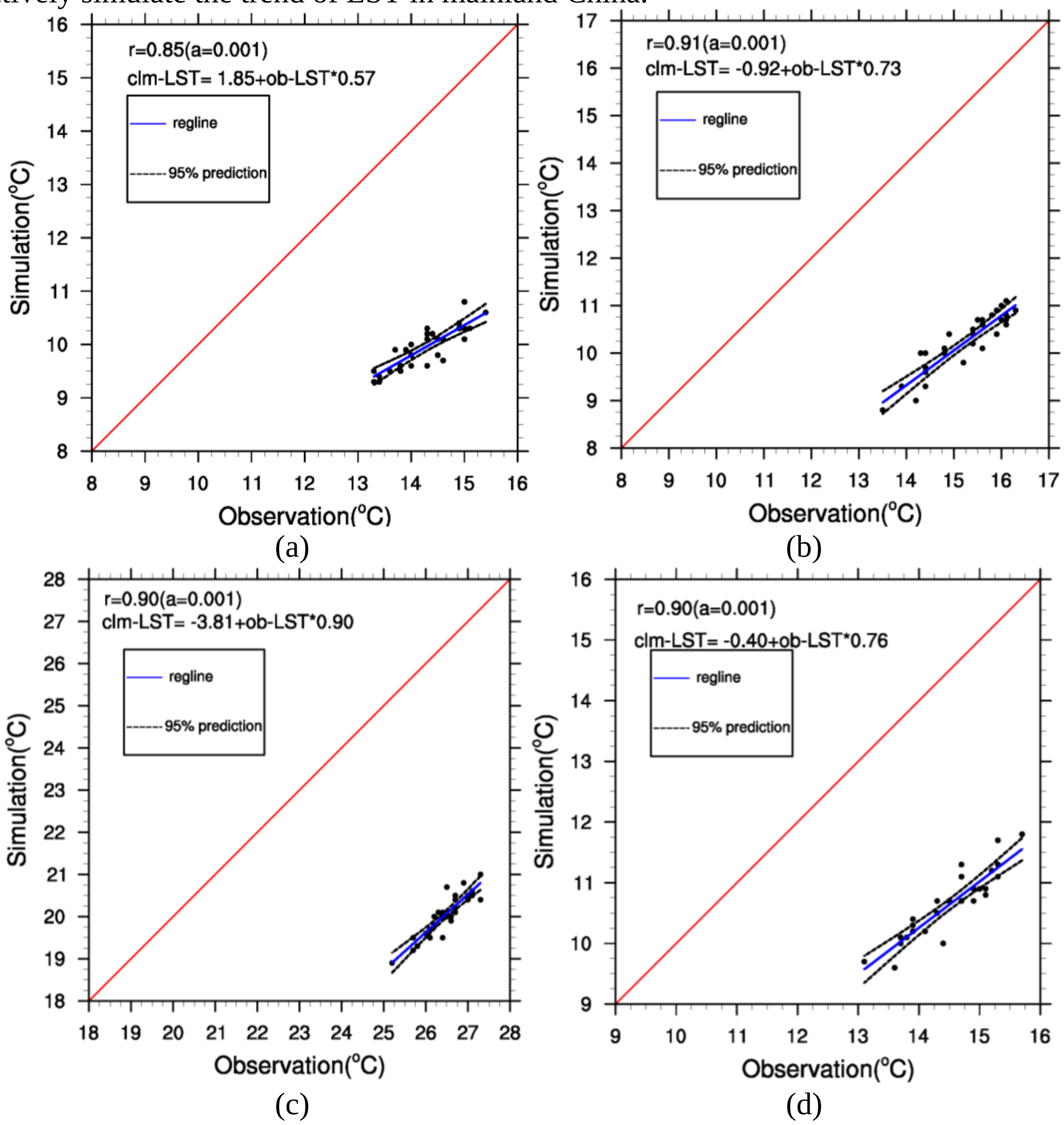

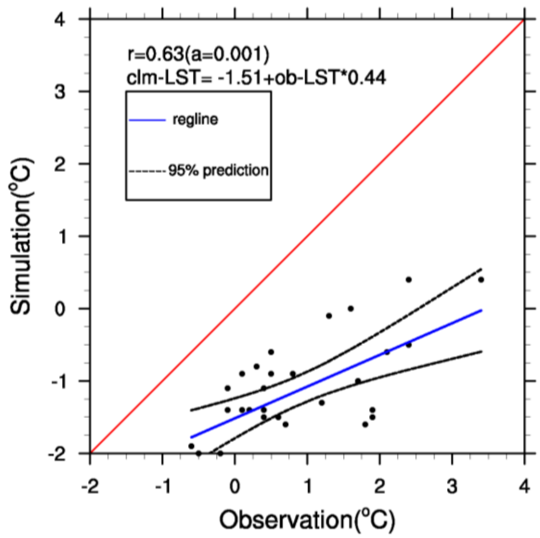

(e)

Fig 9. Correlation and linear regression between observed and simulated LST. (a) regression of regional annual average LST; (b) regression of regional annual spring LST; (c) regression of regional summer average LST; (d) regression of regional autumn average LST; (e) regression of regional winter average LST.

2) Trends

The Theil-Sen (Lavagnini et al. 2011) method was used to analyze the trend of annual average LST in China over the past 30 years. The results show that this temperature increased at a rate of 0.58°C/decade over that period. The plateau and northwestern regions had the maximum increases (0.77 and 0.71°C/decade respectively), while the northern region had little change (0.33°C/decade). LST simulated by CLM4.5 also increased, but the increase was less than observed. In spring, the rate of increase of LST in China was 0.77°C/decade, with that in the plateau region having the maximum increase (1.33°C/decade), and other regions showing small increases. CLM successfully simulated the increasing trend of LST in all regions during spring, but the increase was smaller than observed. Notably, the rapid temperature increase in the plateau region was not reproduced by the simulation. In summer, the LST in all of mainland China increased fastest, at 0.94°C/decade. However, the value simulated by CLM was 0.72°C/decade smaller than observed. The plateau temperature also increased sharply, at 1.33°C/decade, with the simulated value 1.48°C/a smaller than observed. Similar to spring and summer, the trend of LST increase in autumn and winter was accurately simulated, but the simulated increase was smaller than observed (Table 2).

Table 2. Simulation of trend in land surface temperature of mainland China in recent 30 years by CLM4.5 (unit: °C/decade), entire year and seasonally

Period	Product	Entire country	Northwestern	Northern	Southern	Plateau
Year	Ob	0.58	0.71	0.33	0.50	0.77
	CLM4.5	0.29	0.44	0.36	0.25	0.00
	CLM4.5-Ob	-0.29	-0.27	0.03	-0.25	-0.77
Spring	Ob	0.77	0.8	0.50	0.50	1.33
	CLM4.5	0.39	0.53	0.43	0.28	0.10
	CLM4.5-Ob	-0.38	-0.27	-0.07	-0.22	-1.23
Summer	Ob	0.94	1.00	0.74	0.71	1.33
	CLM4.5	0.22	0.47	0.50	0.17	-0.15
	CLM4.5-Ob	-0.72	-0.53	-0.24	-0.54	-1.48

	Ob	0.37	0.62	0.16	0.42	0.29
Autumn	CLM4.5	0.31	0.50	0.27	0.37	0.06
	CLM4.5-Ob	-0.06	-0.12	0.11	-0.05	-0.23
	Ob·	0.67	0.68	0.45	0.67	0.88
Winter	CLM4.5	0.25	0.20	0.39	0.31	0.20
	CLM4.5-Ob	-0.42	-0.48	-0.06	-0.36	-0.68

Comparison of the simulated trend of the three LST products (Table 3) shows that their variations were all smaller than observed. CLM4.5 showed a performance similar to ERA-Interim/Land for annual average variation. Among the regions, the simulated variation of the plateau was the most different from observation, whereas that of the northern region was the best. The simulated variations in the northwestern and southern regions were similar. Seasonally, the simulated variation in autumn was closest to observation, and those in spring and winter were also close. The difference between simulation and observation in summer was the largest.

Table 3. Simulation of trend in land surface temperature of mainland China in recent 30 years by CLM4.5 (unit: °C/decade), entire year and seasonally

Period	Product	Entire country	Northwestern	Northern	Southern	Plateau
Annual	Interim-ob	-0.4	-0.36	-0.1	-0.3	-0.86
	Interim/Land-ob	-0.31	-0.15	-0.04	-0.25	-0.77
MAM	Interim-ob	-0.57	-0.35	-0.17	-0.38	-1.44
	Interim/Land-ob	-0.57	-0.16	-0.13	-0.36	-1.66
JJA	Interim-ob	-0.85	-0.69	-0.36	-0.71	-1.66
	Interim/Land-ob	-0.81	-0.5	-0.14	-0.71	-2.08
SON	Interim-ob	-0.13	-0.2	0	-0.09	-0.21
	Interim/Land-ob	0.03	0.05	-0.02	-0.02	0.11
DJF	Interim-ob	-0.53	-0.54	-0.26	-0.56	-0.8
	Interim/Land-ob	-0.34	-0.08	-0.34	-0.62	-0.35

The Taylor (2001) diagram provides a visual framework for comparing a set of variables from one or more test datasets to one or more reference datasets. In the present work, the diagram was used to comprehensively assess the performance of the three types of simulations of LST in mainland China (Fig. 10). The results show that CLM4.5 was better than the other two types of simulations in winter and the full year (blue solid circles closer to the REF), with its performance intermediate to those of the other two products in the other seasons.

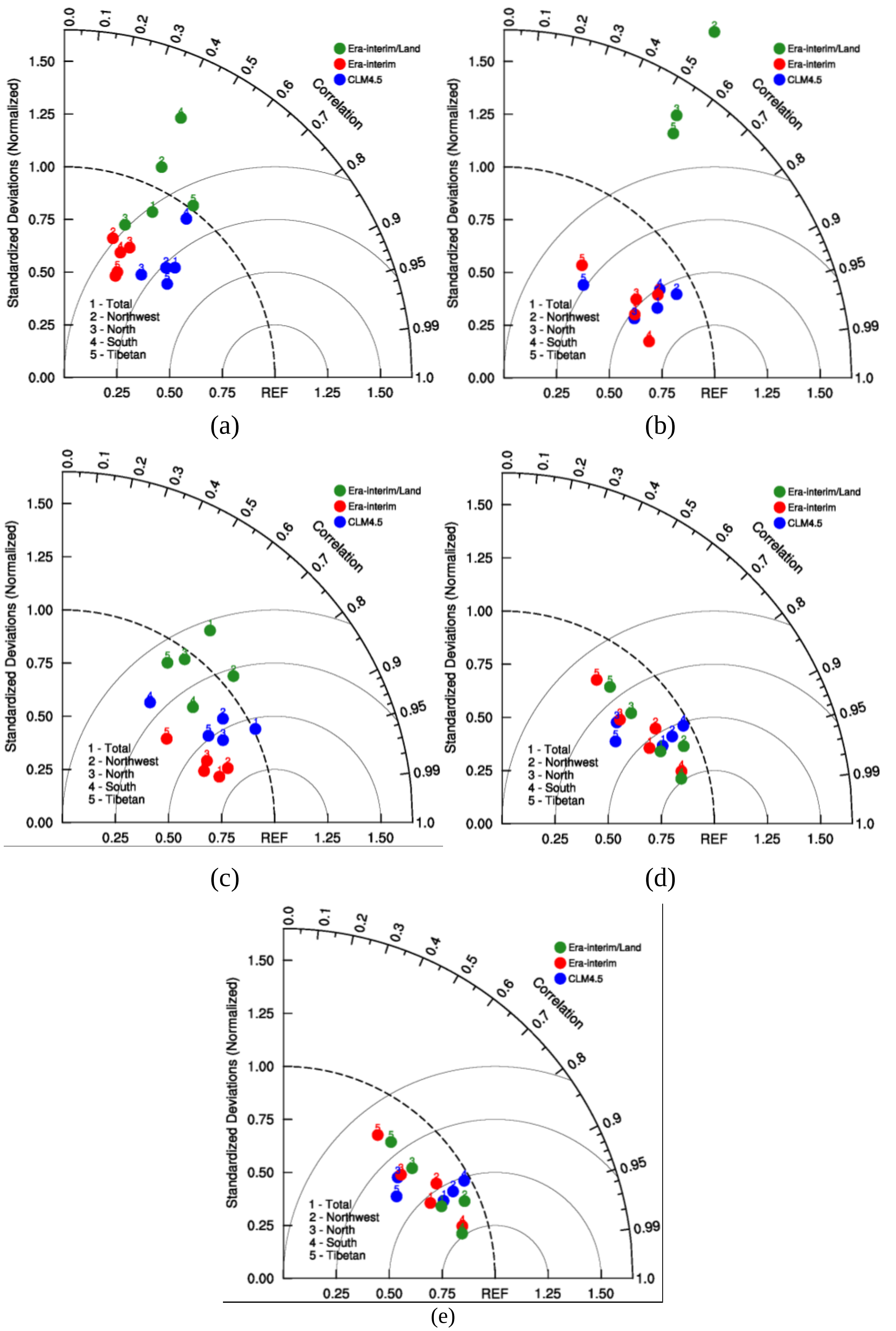

Fig 10. Taylor diagrams of CLM45, EC-interim, and EC-interim/Land

4.2 Improvement of LST simulation

Although CLM4.5 effectively simulated the spatial distribution of LST in the region, there was a cold bias of 4.5°C for all of mainland China. The simulated LSTs were about 2–4°C cooler than observed east of 105°E, and 6–8°C cooler west of 105°E. Bias of the Tibetan Plateau was maximum among the regions, with an annual average cold bias of ~6°C. Maybe the model of the thermal conductivity in CLM4.5 is the main reason. To study the effect of STC (λ) on the simulation of LST, two long-term (30-year) simulation tests were conducted for two schemes. The results shows that the LST in most of northern China simulated by the Côté-Konrad scheme was increased by 0.5–1.0°C over that of the Johansen scheme, whereas that temperature in most other regions was reduced by 0–0.5°C (Fig. 11a). In the Lu-Ren scheme, LST was increased by 0.5–1.0°C over that of Johansen scheme in most regions except the Tibetan Plateau and Guangdong and Guangxi regions, where that temperature was reduced by 0–0.5°C. LST in most of northern China was increased by 1–1.5°C, with the increase in some areas reaching 3°C (Fig. 11b).

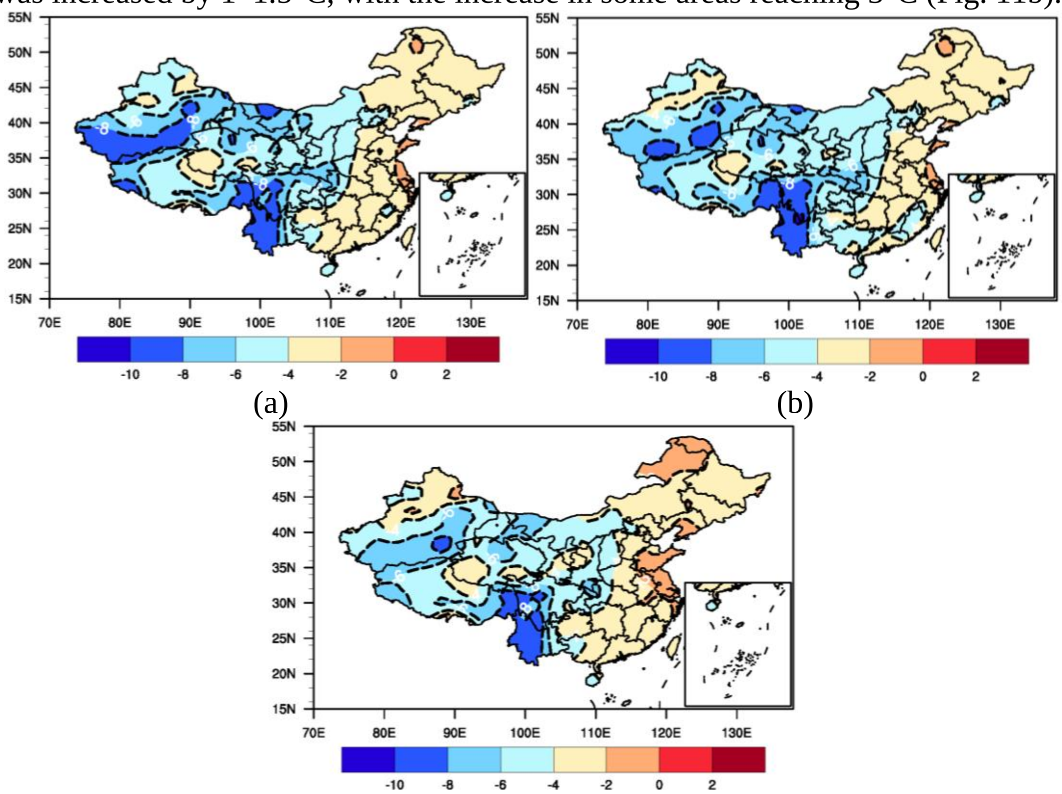

Fig 11. Bias of LST values simulated by the Côté-Konrad (2005) and Lu-Ren (2006) schemes from the values simulated by the Johansen (1975) scheme; unit: °C.

According to the bias of the three schemes, there is little difference between the Johansen and the Côté-Konrad scheme(Fig.12a). While the Lu-Ren scheme can significantly reduce the cold deviation in most regions. Therefore, it is more suitable for Chinese mainland LST simulation(Fig.12b).

On the other hand, the bias in summer and autumn was greater than in other seasons. Because of the heavy rainfall, the soil moisture in these two seasons is higher than that in other periods. While the soil moisture change had an important effect on the simulation of LST, especially in arid and semiarid areas of northern China, where evaporation at the soil surface is intense. However, the isothermal model used in CLM4.5 did not consider the effect of soil moisture change on soil temperature, maybe resulting in a large simulated bias in northern and northwestern regions with low soil moisture and large soil moisture variation. Therefore, developing a new λ calculation scheme and considering the role of water vapor in the calculation model of soil temperature are effective means for improving the performance of the model in simulating LST in mainland China.

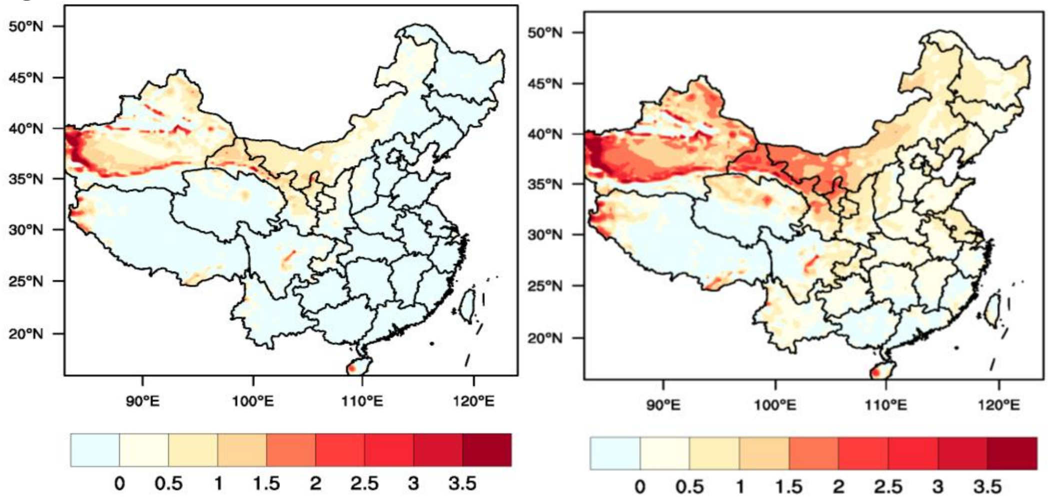

(a) (b)

Fig 12. Bias of LST values simulated by the Côté-Konrad (2005) and Lu-Ren (2006) schemes, unit: °C.

5 Conclusions

We ran the CLM4.5 in a land–atmosphere coupling approach. And the longest and latest observed LST dataset for mainland China was used for the first time to comprehensive assess LST in that region as simulated by CLM4.5. The results show that there are systematic cold deviations in the simulation of land surface temperature in mainland China by CLM4.5. The RMSE in mainland China increased gradually from southeast to northwest, with the smallest value in the south (1–3°C) and largest in the southern Xinjiang Basin (9–11°C). Summer and autumn had the smallest RMSEs for each region in a year. Correlation coefficients between simulation and observation for all stations in China were between 0.75 and 0.9 ($P < 0.001$). The strongest correlation was observed in summer, with the correlation coefficient from 0.70 to 0.85 ($P < 0.001$). In winter, that coefficient was the smallest, 0.35 to 0.65 ($P < 0.05$). As a result, the observed annual and seasonal average LSTs in mainland China had strong linear relationships with those simulated by CLM4.5. In the past 30 years, the LST of mainland China increased at the rate 0.058°C/a, with that of the plateau and northwestern regions increasing fastest (0.077 and 0.071°C/a, respectively) and that in the northern region changing the least (0.033°C/a). The LST simulated by CLM4.5 also increased, but that increase was smaller than observed.

The STC sensitivity numerical tests show that STC had a major influence on the reduction of simulated LST. However, the simulated cold bias from the Lu-Ren scheme remained large, and there was an increasing trend of the bias for the Tibetan Plateau. In addition, the bias in summer and autumn was greater than in other seasons, which shows that soil moisture change had an important effect on the simulation of LST, especially in arid and semiarid areas of northern China, where evaporation at the soil surface is intense. However, the isothermal model used in CLM4.5 did not consider the effect of soil moisture change on soil temperature, resulting in a large simulated bias in northern and northwestern regions with low soil moisture and large soil moisture variation. Therefore, developing a new λ calculation scheme and considering the role of water vapor in the calculation model of soil temperature are effective means for improving the performance of the model in simulating LST in mainland China.

Overall, although CLM4.5 can effectively simulated the spatial distribution and the variation of LST in the region.there exists larger cold bias for all of mainland China. The introduction of soil thermal conductivity model considering soil moisture may reduce the simulation deviation.

Acknowledgments, Samples, and Data

- This research was funded by by the China Meteorological Administration Special Public Welfare Research Fund (GYHY 201506001) , National Natural Science Foundation of China (41805079), and Innovation Team of Gansu Meteorological Bureau (GSQXCXTD-2020-01).
- The authors declare no conflict of interest.
- Climate data were downloaded from http://data.cma.cn/user/toLogin.html, ERA-5 data were download from https://software.ecmwf.int/wiki/display/WEBAPI/.

References

Akkermans, T., Thiery, W., Van Lipzig, N. P. M.(2014), The regional climate impact of a realistic future deforestation scenario in the congo basin. *J.Climate*, ***27*(7)**,2714-2734,doi: 10.1175/JCLI-D-13-00361.1.

Bilionis, I., Drewniak, B. A., Constantinescu, E. M.(2014), Crop physiology calibration in clm. *Geoscientific Model Development Discussions*, ***7*(5)**,1071-1083,doi:10.5194/gmdd-7-6733-2014.

Balsamo, G., Albergel, C., Beljaars, A.,et al.(2015), ERA-Interim/Land: a global land surface reanalysis data set, Hydrol. *Earth Syst. Sci.*, **19**, 389-407, doi:10.5194/hess-19-389-2015.

Brunke, M. A., Broxton, P., Pelletier, J., et al.(2016), Implementing and evaluating variable soil thickness in the community land model version 4.5 (clm4.5). *J. Climate*, ***29*(9)**, 3441-3461,doi: 10.1175/jcli-d-15-0307.1.

Côté,J., Konrad,J.M.(2005), A generalized thermal conductivity model for soils and construction materials. *Canadian Geotechnical Journal*, **42(3)**,443-458.

Chen,H.S.,Xiong,M.M.,Sha,W.Y.(2010), Simulation of land surface processes over China and its validation Part I:Soil temperature. *Scientia Meteorologica Scinica*,**30(5)**,621-630,doi:10.3969/j.issn.1009-0827.2010.05.008.

C. Albergel, W. Dorigo, R. H., Reichle, G. et al.(2013), Skill and Global Trend Analysis of Soil Moisture from Reanalyses and Microwave Remote Sensing. *J. Hydrometeor.*, **14**, 1259–1277, doi:10.1175/JHM-D-12-0161.1.

Coll,C., Garciasantos,V., Niclos,R.(2016),Test of the MODIS Land Surface Temperature and Emissivity Separation Algorithm With Ground Measurements Over a Rice Paddy[J]. *IEEE Trans. Geosci. Remote Sens.*, **54(5)**,3061-3069.

Chen, M., Griffis, T. J., Baker, J. M., et al.(2018),Comparing crop growth and carbon budgets simulated across ameriflux agricultural sites using the community land model (clm). *Agricultural and Forest Meteorology*, **256-257**,315-333,doi: 10.1016/j.agrformet.2018.03.012.

Duan, S. B., Li, Z. L., Leng, P.(2017), A framework for the retrieval of all-weather land surface temperature at a high spatial resolution from polar-orbiting thermal infrared and passive microwave data. *Remote Sens. Environ.*, **195**:107-117,doi: 10.1016/j.rse.2017.04.008.

Duarte, H. F., Raczka, B. M., Ricciuto, D. M. et al.(2017), Evaluating the community land model (clm4.5) at a coniferous forest site in northwestern united states using flux and carbon-isotope measurements. *Biogeosciences*, **14(18)**, 4315-4340,doi: 10.5194/bg-14-4315-2017.

Fu, C., Wang, G., Goulden, M. L.,et al.(2016), Combined measurement and modeling of the hydrological impact of hydraulic, redistribution using clm4.5 at eight ameriflux sites. *Hydrology and Earth System Sciences*, ***20*****(5)**, 2001-2018,doi: 10.5194/hess-20-2001-2016.

Guo,D.L., Li,D., Liu,G.Y.(2017),Simulated change in soil temperature on the Tibetan Plateau from 1901 to 2010. *Quaternary Sciences*,**37(5)**:1102-1110,doi:10.11928/j.issn.1001-7410.2017.05.17.

Guo, D., Wang, A., Li, D.,et al.(2018), Simulation of changes in the near-surface soil freeze/thaw cycle using clm4.5 with four atmospheric forcing datasets. *J.Geophys.Res.*,**123**,doi: 10.1002/2017JD028097.

Huang, B.W.(1989), Outline of China's Comprehensive Natural Zoning. *Geography*, **21**, 10-20.

Hoffman, F., Vertenstein, M., Thornton, P.,et al.(2004), Community land model version 3.0 (clm3.0) developer’s guide. *J.Climate*.doi: 10.2172/885637.

Hack, J. J., Caron, J. M., Yeager, S. G., et al.(2006), Simulation of the global hydrological cycle in the ccsm community atmosphere model version 3 (cam3): mean features. *J. Climate*, **19(11)**, 2199-2221,doi: 10.1175/jcli3755.1.

Huszár, Peter, Karlicky, J., et al.(2018), The impact of urban canopy meteorological forcing on summer photochemistry. *Atmos.Environ.*, **176**,209-228,doi, 10.1016/j.atmosenv.2017.12.037.

Johansne,O.,1975,Thermal Properities of Soils.Ph.D.thesis,University of Trondheim.

Jones, D. A., Trewin, B. C.(2015), On the relationships between the El Niño-Southern Oscillation and Australian land surface temperature. *Int. J. Climatol*,**20(7)**,697-719.doi,0.1002/1097-0088(20000615)20,7<697,,AID-JOC499>3.0.CO;2-A.

Kohnemann, S.H.E., Heinemann, et al.(2017), Extreme warming in the kara sea and barents sea during the winter period 2000 to 2016. *J. Climate*, **30(22)**, 8913-8927,doi,10.1175/JCLI-D-16-0693.1.

Lu,S.,Ren, T.,Gong,Y.S.(2006), An improved model for predicting soil thermal conductivity from water content at room temperature[J]. *Soil Science Society of America Journal*, **71(1)**,8-14,doi, 10.2136/sssaj2006.0041.

Lavagnini, I., Badocco, D., Pastore, P. et al.(2011), Theil–sen nonparametric regression technique on univariate calibration, inverse regression and detection limits. *Talanta*,**87**, 0-188,doi, 10.1016/j.talanta.2011.09.059.

Li, H., Huang, M., Wigmosta, M.S.,et al.(2011), Evaluating runoff simulations from the community land model 4.0 using observations from flux towers and a mountainous watershed. *J. Geophys. Res.*, **116,** D24120,doi, 10.1029/2011JD016276.

Lawrence, D.M., Slater, A.G., Swenson, S.C.(2012), Simulation of present-day and future permafrost and seasonally frozen ground conditions in ccsm4. *J.Climate*, ***25*****(7)**, 2207-2225.doi, 10.1175/JCLI-D-11-00334.1.

Lai, X., Wen, J., Ceng, S.X., et al.(2014), Numerical simulation and evaluation study of soil moisture over china by using clm4.0 model [in chinese]. *J. Atmos. Sci.*, **38(3)**, 499-512,doi, 10.3878/j.issn.1006-9895. 1401.13194.

Liu, D., Mishra, A.K.(2017),Performance of amsr_e soil moisture data assimilation in clm4.5 model for monitoring hydrologic fluxes at global scale. *J.Hydrol.,* **547**,67-79,doi, 10.1016/j.jhydrol.2017.01.036.

Meng, C., Zhang, C., Tang, R.(2013), Variational estimation of land–atmosphere heat fluxes and land surface parameters using modis remote sensing data. *J. Hydrol.,* **14(2)**, 608-621,doi, 10.1175/JHM-D-12-028.1.

Ming, S.Y., Yi, F., Jiao, M.T.(2014), Evaluation of simulation performance of land surface model ncar_clm4.5 at a degrated glassland station in semi-arid area. *Transactions of Atmospheric Sciences*.,**37(6)**,794-803 (in Chinese), doi, 10.13878/j.cnki.dqkxxb.20140105001.

Meng, X., Wang, H., Wu, Y.,et al.(2017), Investigating spatiotemporal changes of the land-surface processes in xinjiang using high-resolution clm3.5 and cldas, soil temperature. *Scientific Reports,* **7(1)**, 13286, doi, 10.1038/s41598-017-10665-8.

Meng,X.Y., Wang, H., Liu, Z.H., et al.(2017), Simulation and verification of land surface soil temperatures in the Xinjiang Region by the CLM3.5 model forced by CLDAS. *Acta Ecologica Sinica*, **37(3)**, 979-995, doi,10.5846/stxb201508171717.

Peng, B., Guan, K., Chen, M., et al.(2018), Improving maize growth processes in the community land model, implementation and evaluation. *Agricultural and Forest Meteorology,* **250-251**, 64-89,doi, 10.1016/j.agrformet.2017.11.012.

Su,L.J., Wang,Q.J., Wang,S.,et al.(2016), Soil thermal conductivity model based on soil physical basic parameters.*Transactions of the CSAE*.,**32(2)**,127-133,doi,10.11975/j.issn.1002-6819.2016.02.019.

Sun,S., Shi, C.S.,Liang, X., et al.(2017), Assessment of Ground Temperature Simulation in China by Different Land Surface Models Based on Station Observations. *J. Appl. Meteor*., **28(6)**,737-749,doi,CNKI,SUN,YYQX.0.2017-06-009.

Sheng, M., Liu, J., Zhu, A.X.,et al.(2018), Evaluation of clm-crop for maize growth simulation over northeast china. *Ecological Modelling,* **377,** 26-34,doi, 10.1016/j.ecolmodel.2018.03.005.

Taylor, Karl, E.(2001),Summarizing multiple aspects of model performance in a single diagram. *J. Geophys. Res.*, **106(D7)**, 7183,doi, 10.1029/2000jd900719.

Tang, J., Riley, W.J., Niu, J.(2015),Incorporating root hydraulic redistribution in CLM4.5, Effects on predicted site and global evapotranspiration, soil moisture, and water storage. *Journal of Advances in Modeling Earth Systems*, **7(4)**,1828-1848,doi, 10.1002/2015MS000484.

Tran, D.X., Pla, F., Latorre-Carmona, P.,et al.(2017), Characterizing the relationship between land use land cover change and land surface temperature. *ISPRS Journal of Photogrammetry and Remote Sensing,* **124**,119-132,doi, 10.1016/j.isprsjprs.2017.01.001.

Umair, M., Kim, D., Ray, R.L., et al.(2018), Estimating land surface variables and sensitivity analysis for clm and vic simulations using remote sensing products. *Science of The Total Environment,* **633**, 470-483.,doi, 10.1016/j.scitotenv.2018.03.138.

Wan, Z., Li, Z.L.(1997),A physics based algorithm for retrieving land‐surface emissivity and temperature from EOS/MODIS data. *IEEE Trans. Geosci. Remote Sens.*,**35**,980-996.

Wilson, J. S., Clay, M., Martin, E., et al.(2003), Evaluating environmental influences of zoning in urban ecosystems with remote sensing. *Remote Sens. Environ.*, **86(3)**,303-321,doi,10.1016/s0034-4257(03)00084-1.

Wu,W., Dickinson,R.E. et al.(2004),Time scales of layered soil moisture memory in the context of land-atmosphere interaction. *J.Climate*, **_17_(14)**,2752-2764,doi,10.1175/1520-0442(2004)017<2752,tsolsm>2.0.co;2.

Wang,X.Fj., Yang, M.X., Guo, J.P.(2015), Simulation and improvement of land surface processes in Nameqie, Central Tibetan Plateau, using the Community Land Model (CLM3.5). *Environmental Earth Sciences*, **73(11)**,7343-7357,doi, 10.1007/s12665-014-3911-4.

Wood, E., Siemann, A., Coccia, G.,et al.(2016),Development and Analysis of a Long Term, Global, Terrestrial Land Surface Temperature Dataset Based on HIRS Satellite Retrievals. *Egu General Assembly Conference*. EGU General Assembly Conference Abstracts.

Xie, Z.P.,Hu,Z.Y.,Liu,H.L.(2017), Evaluation of the Surface Energy Exchange Simulations of Land Surface Model CLM4.5 in Alpine Meadow over the Qinghai-Xizang Plateau. *Plateau Meteor*., 36(1),1-12, doi,10.7522/j.issn.1000-0534.2016.00012.

Yuan, X., &Zhu, E.(2018), A first look at decadal hydrological predictability by land surface ensemble simulations. *Geophys. Res. Lett*., 45, 2362–2369. doi,10.1002/2018GL077211.

Zhang, Y., &Wang,W.C.(1997), Model simulated northern winter cyclone and anticyclone activity under a greenhouse warming scenario. *J.Climate*, 10(7),1616-1634,doi, 10.1175/1520-0442(1997)010<1616,MSNWCA>2.0.CO;2.

Zeng, X., Shaikh, M., Dai, Y., et al.(2002),Coupling of the common land model to the ncar community climate model. *J.Climate*, 15(14),1832-1854.doi, 10.1175/1520-0442(2002)015<1832,cotclm>2.0.co;2.

Zhong, L., Su, Z., Ma, Y.,et al.(2011),Accelerated changes of environmental conditions on the tibetan plateau caused by climate change. *J. Climate*, 24(24), 6540-6550,doi,10.1175/jcli-d-10-05000.1.

Zhang, L., Mao, J., Shi, X., et al.(2016), Evaluation of the community land model simulated carbon and water fluxes against observations over chinaflux sites. *Agricultural and Forest Meteorology*, **226-227**,174-185,doi, 10.1016/j.agrformet.2016.05.018.